Preparation and application of coconut shell-based skeleton particles coupled with hydroxypropyltrimethyl ammonium chloride chitosan in sludge dewatering

Shici Zhang[a,b,c,†], Ying Zhang[a,d,†], Haohan Xu[e], Qi Liu[b], Xiang Wan[c], Jiajia Xia[a], Longkai Li[a], Hui Zhang[a,b,*], Xujie Lu[f,*]

[a]Hubei Key Laboratory of Industrial Fume and Dust Pollution Control, School of Environment and Health, Jianghan University, Wuhan 430056, China, emails: zhanghui@jhun.edu.cn (H. Zhang), zhangshici@jhun.edu.cn (S. Zhang), anna.zhang@163.com (Y. Zhang), xiajiajia8@qq.com (J.J. Xia), longkai_li@qq.com (L.K. Li)
[b]Central and Southern China Municipal Engineering Design and Research Institute Co., Ltd., Wuhan 430010, China, email: amuliuqi@qq.com (Q. Liu)
[c]Hubei Geological Survey, Wuhan 430034, China, email: wxzgdz@webmail.hzau.edu.cn (X. Wan)
[d]School of Medicine, Xiangyang Polytechnic, Xiangyang 441050, China
[e]Institute of Soil Environment, Hubei Provincial Academy of Eco-Environmental Sciences, Wuhan 430070, China, email: xuhaohan2000@foxmail.com (H.H. Xu)
[f]Yazhouwan Innovation Research Institute of Hainan Tropical Ocean University, Sanya 572022, China, email: xujie_lu@163.com (X.J. Lu)

ABSTRACT

The sludge dewatering is a significant part of municipal wastewater treatment industry, and efficient disposal techniques for the sludge dewatering is still a challenge among worldwide environmental fields. To achieve sludge reduction, the research and exploitation of environment-friendly natural polymer dehydrating agents have caused broad attention. In this study, a coconut shell-based composite was prepared by grafting hydroxypropyltrimethyl ammonium chloride chitosan (HACC) on the surface of coconut shell skeleton particles as a novel type of dewatering agent. The response surface methodology was used to optimize the preparation process of grafted coconut shell-based skeleton particles. The consumption per unit area of HACC could reach 0.1732 g/g under the optimal preparation conditions: reaction temperature at 40°C, material particle size at 120–200 mesh, mass ratio of M1:M2 at 0.75 without dilution, and ultrasonic time for 5 min. Compared to the composites without graft, the dewatering rate of sludge was obviously improved by the grafted coconut shell-based composites under the same treatment procedures. Moreover, the grafted coconut shell-based composite also possessed the potential for effectively adsorbing the total organic matters in sludge dewatering filtrate. This work provides a promising dehydrating agent and disposal method for the practical application of municipal sludge dewatering.

Keywords: Coconut shell; Skeleton particles; Hydroxypropyltrimethyl ammonium chloride chitosan; Sludge dewatering; Response surface methodology

* Corresponding authors.
† Co-first authors.

1. Introduction

With the acceleration of the scale of urban sewage treatment, the number of newly built and renovated urban sewage treatment plants has surged. Up to 2019, China was estimated to possess more than 5000 municipal wastewater treatment plants (WWTPs), while the output of sludge (calculated at a moisture content of 80%) approached 60 million tons each year [1,2]. As a by-product of municipal wastewater treatment, the municipal sludge has complex components and usually contains a large number of pathogenic bacteria, refractory organic matter, microplastics and toxic heavy metals, which brings huge pressure to the sustainable development of the ecological environment [3,4]. Dewatering seems to be an alternative approach to impel the treatment and reuse of sludge. The excess sludge has high hydrophilicity, biogel structure, and large surface area, resulting in a strong binding force between the sludge water (surface adsorbing water and chemical bonding water) and the particles [5,6], and further leading to a sludge's moisture content remaining at about 80%–85% after conventional dewatering, or even much higher [7]. The cost of subsequent disposal and resource utilization of sludge are difficult to meet the requirements of sanitary landfill, incineration, agricultural use, and building materials manufacturing also due to the high moisture content of sludge [8,9]. Deep dewatering has become the bottleneck of sludge disposal in municipal wastewater treatment industry, and it is also an urgent need to achieve the goal of "low-carbon development" for worldwide countries [10].

Sludge conditioning technology is the key factor for deep sludge dewatering. Thereinto, chemical conditioning is widely used for high-efficiency sludge conditioning, including oxidation conditioning and flocculation conditioning [11]. Polyaluminum chloride (PAC) was the most common flocculant in industrial sludge dewatering [12]. However, chemical conditioning results in higher sludge compressibility, and dewatering efficiency is largely limited by filter media and filter cakes [4,13]. Studies have shown that the skeletal materials are used to combine with the oxidants or flocculants to condition the sludge, and further increase the rigid structure and water permeability, thereby improving the dewatering performance and effect of the sludge [7]. Inert materials such as fly ash [14], quicklime [15], phosphogypsum [16,17], lignite [13], and crop straws [18] are used as skeleton particles to form a hard and dense skeleton structure in the sludge, which reduces the compressibility of the sludge and ensures the dewatering effect [19,20]. However, some minerals, especially fly ash, contain a certain amount of heavy metals and other harmful substances [21]. Introduce exogenous hazardous constituents into the sludge system may generate secondary pollution, and further cause ecological environment and human health risks, as well as different impacts on subsequent treatment and disposal. Therefore, non-toxic and natural biomass materials show great potential for sludge conditioning, such as rice husk [22], walnut shell [23], bamboo powder [24], wheat straw powder [25], corn-core powder [26], and other materials. With the conditioning of biomass materials, the calorific value and organic matter content of the sludge could be markedly improved, which is beneficial to the subsequent incineration of sludge, composting, sludge biochar preparation and other resource applications [27,28].

Coconut shell is an ubiquitous agricultural by-product in tropical regions [29]. Due to the well-developed pore structure inside, most coconut shells are used to prepare activated carbon or biochar granules/powder, which requires additional investment for hydrothermal or calcination preparation [30,31]. At present, there are few studies on the direct application of coconut shell without secondary operation. Coconut shell, as a common lignocellulosic biomass material, theoretically possesses the potential to be used for sludge dewatering [32–34]. Additionally, in the current sludge dewatering process, the combined use of flocculants and biomass has been paid much attention due to the synergic effect, while the research on grafting flocculants to prepare biomass based skeleton particles is relatively rare [35,36]. Hydroxypropyltrimethyl ammonium chloride chitosan (HACC) is a kind of water-soluble cationic chitosan with good biocompatibility, hydrophilicity and antimicrobial activity, which could enhance the performance of sludge dewatering based on biomass [37,38]. To improving the sludge dewatering efficiency, it is of great significance to study the optimal condition of grafting HACC on biomass.

Based on the above-discussion, a novel type of sludge dewatering composite was successfully prepared by grafting HACC on the surface of coconut shell skeleton particles in this study. The purposes of this research were proposed as follows: (1) using response surface methodology (RSM) to optimize the HACC grafting conditions on the surface of coconut shell skeleton particles; (2) comparing the performance of coconut shell-based skeleton particles and traditional flocculant (PAC) for sludge dewatering; (3) evaluating the total nitrogen (TN) and total organic carbon (TOC) removal performance during sludge dewatering.

2. Materials and methods

2.1. Materials and instruments

2.1.1. Materials

Coconut shell was collected from the local fruit market and activated sludge was provided by the local sewage treatment plant in Hainan Province. Silane coupling agent (KH-560) was purchased from Shandong Yousuo Chemical Co., Ltd., (China). HACC and PAC were purchased from Aladdin Co., Ltd., (China). All reagents were used directly without further purification. All solutions used in this work was configured with ultrapure water (DW, 18.2 MΩ/cm, Milli-Q).

2.1.2. Instruments

An ultraviolet-visible spectrophotometer (UV752N) was used to analyze the concentration of HACC and TN in the solution. An ultrasonic oscillator (SB-5200) was used to assist the HACC grafting process. Total organic carbon analyzer (multi N/C 3100) was used to analyze TOC content in sludge filtrate. Biological microscope (BM1000) and stereo microscope (SE2200) were used to observe the

status of sludge dewatering. A super-resolution field emission scanning electron microscope (SU8010) was used to observe the coconut shell-based skeleton particles.

2.2. Prepared of HACC grafted coconut shell-based skeleton particles

Coconut shell was ground using a crusher, and then sieved with different mesh sizes. The obtained solid substances were coconut shell-based skeleton particles, denoted as CSBSP. The RSM was used to optimize the preparation process of grafted coconut shell-based skeleton particles (denoted as GCSBSP) as shown in Table 1. Experiments were designed and optimized according to the Box–Behnken design principle using Design–Expert software. The effect of temperature, particle size and material ratio (CSBSP:HACC denoted as M1:M2) on the consumption per unit area of HACC was investigated. The experimental section for the preparation of GCSBSP was as follows: 100 mL of 1 g/L HACC solution, 40 μL of silane coupling agent and a certain mass of CSBSP were added into the beaker. The beaker was placed on an ultrasonic oscillator for 5 min. After that, a portion of the upper liquid in the beaker was extracted into a centrifuge tube and centrifuged at 8,000 rpm for 15 min. Then, the supernatant was further extracted to measure the remaining concentration of HACC. The HACC content in the solution was determined using spectrophotometry

Table 1
Analysis of factors and levels by response surface methodology

Factor	Level		
	−1	0	1
A (Temperature, °C)	30	40	50
B (particle size, mesh)	60–120	120–200	>200
C (Material ratio, M1:M2)	0.5	0.75	1

method at a wavelength of 518 nm. The cost quantity of HACC on grafting was calculated according to the initial and remaining content of HACC. Fig. 1 indicates the possible graft mechanism diagram of HACC on CSBSP. The polysaccharide content, such as cellulose, hemicellulose and lignin, could grafted on the surface of CSBSP by substitution reaction.

2.3. Performance evaluation of dewatering agent

Sludge dewatering performance test was employed using vacuum filtration device. Transfer 300 mL of activated sludge into a 500 mL beaker, and then a certain mass of PAC/CSBSP/GCSBSP was added, followed by stirring at 180 rpm for 5 min. After that, the sludge mixture was introduced into a Buchner funnel for vacuum filtration, and the vacuum gauge pressure, filtration time and filtrate volume were recorded during the filtration process. Finally, the mud cake was taken to measure the moisture content, solid content, wet and dry weight of the sludge. Another dewatering method, mechanical centrifuge was carried out as follows: 6 mL of activated sludge was transferred to a plastic test tube, and then a certain amount of dewatering agent (CSBSP/GCSBSP) was added. The plastic test tubes were capped, shaken well, and centrifuged for 5 min at 4,000 rpm. After that, moisture content of the sludge mixture was calculated by the method of drying weight loss. TN and TOC concentrations in the supernatant after centrifugation were measured using alkaline potassium persulfate digestion UV spectrophotometry [39] and high temperature combustion method [20], respectively. The specific resistance of the sludge was measured by the Buchner funnel method. The moisture content before and after the suction filtration was measured, and the variation curves of filtration time vs. the filtration volume were plotted. According to Eqs. (1) and (2), the specific resistance of the sludge was obtained.

$$b = \frac{\Delta t}{\Delta V} = \frac{\mu \alpha C}{2PF^2} \tag{1}$$
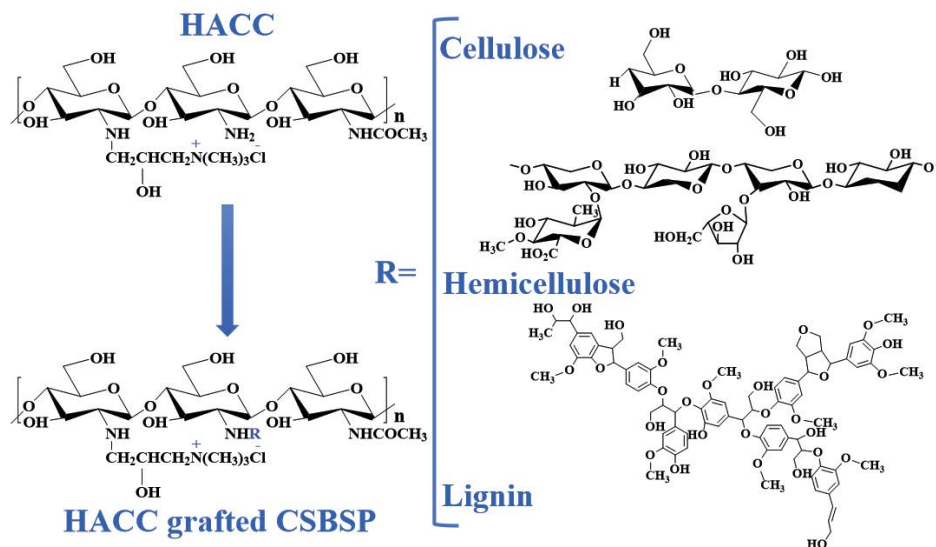

Fig. 1. Possible graft mechanism diagram of hydroxypropyltrimethyl ammonium chloride chitosan on CSBSP.

$$\alpha = \frac{2PF^2}{\mu} \times \frac{b}{c} \qquad (2)$$

where b is the curve slope of filtrate time and filtration volume; α is the sludge specific resistance, s²/g; P is the filtration pressure, MPa; F is the filtration area, cm²; μ is the dynamic viscosity of the filtrate, g·s/cm²; C is the ratio of dry solid weight retained on filter medium to filtrate, g/mL.

3. Results and discussion

3.1. Response surface analysis for the preparation of GCSBSP

Table 2 shows the Box–Behnken experimental design and results for response surface analysis. According to the obtained data, multiple regression analysis was performed using Design–Expert 8.0.6 software. Multivariate quadratic regression equation between response variables (reaction temperature A, material particle size B, material ratio C) and response value (cost) was obtained: Cost = 0.15 − 0.002 041A + 0.042B + 0.002439C + 0.003415AB + 0.080AC − 0.022BC − 0.023A^2 − 0.028B^2 − 0.037C^2.

The significance of the linear relationship between each factor and the response value was determined by the F-value test. The smaller the P-value, the higher the significance of the variable. According to the analysis of variance (Table 3), the linear relationship between the dependent and all independent variables were significant ($r = 0.0122$), and the significant level of the model was 0.5297 (much greater than 0.05), indicating the regression variance model was not significant. The significance order relied on the cost was ranked as: material ratio > reaction temperature > particle size.

With the fixed material ratio of 1:1, the interaction and contour lines of reaction temperature and material mesh is shown in Fig. 2a and b, respectively. The contour map was elliptical. The axial contour for material mesh was dense while for reaction temperature was sparse, indicating that the material mesh had a more obvious impact

on the cost. Under the optimal reaction conditions as follows: the material mesh was 120–200 and the temperature was 40°C, the obtained cost was about 0.16. With the fixed material mesh of 120–200 mesh, the interaction and contour lines of reaction temperature and material ratio is shown in Fig. 2c and d, respectively. The axial contour for material ratio was dense while for reaction temperature was sparse, indicating that the material ratio had a more obvious impact on the cost. Under the optimal reaction conditions as follows: the material ratio was 0.75:1 and the temperature was 40°C, the obtained cost was approximately 0.15. In addition, the interaction and contour lines of material mesh and ratio is shown in Fig. 2e and f with

Table 2
Box–Behnken experimental design and results

Code	A	B	C	Cost
1	−1	−1	0	0.0653
2	1	−1	0	0.0371
3	−1	1	0	0.1532
4	1	1	0	0.1387
5	−1	0	−1	0.1660
6	1	0	−1	0.0191
7	−1	0	1	0.0008
8	1	0	1	0.1741
9	0	−1	−1	0.0191
10	0	1	−1	0.1361
11	0	−1	1	0.0787
12	0	1	1	0.1061
13	0	0	0	0.2926
14	0	0	0	0.0140
15	0	0	0	0.1017
16	0	0	0	0.1900
17	0	0	0	0.1545

Table 3
Analysis of variance

| Source	Sum of squares	Degrees of freedom	Mean square	F-value	Prob. > F
Model	5.500E-02	9	6.057E-03	9.7E-01	0.5297
A	3.333E-05	1	3.333E-05	5.3E-03	0.9439
B	1.400E-02	1	1.400E-02	2.2E+00	0.1794
C	4.759E-05	1	4.759E-05	7.6E-03	0.9330
AB	4.666E-05	1	4.666E-05	7.5E-03	0.9336
AC	2.600E-02	1	2.600E-02	4.1E+00	0.0827
BC	2.010E-03	1	2.010E-03	3.2E-01	0.5886
A^2	2.325E-03	1	2.325E-03	3.7E-01	0.5615
B^2	3.414E-03	1	3.414E-03	5.5E-01	0.4842
C^2	5.786E-03	1	5.786E-03	9.2E-01	0.3683
Residual	4.400E-02	7	6.258E-03		
Loss of quasi-item	1.049E-03	3	3.498E-04	3.3E-02	0.9909
Net error	4.300E-02	4	1.100E-02		
Gross difference	9.800E-02	16			
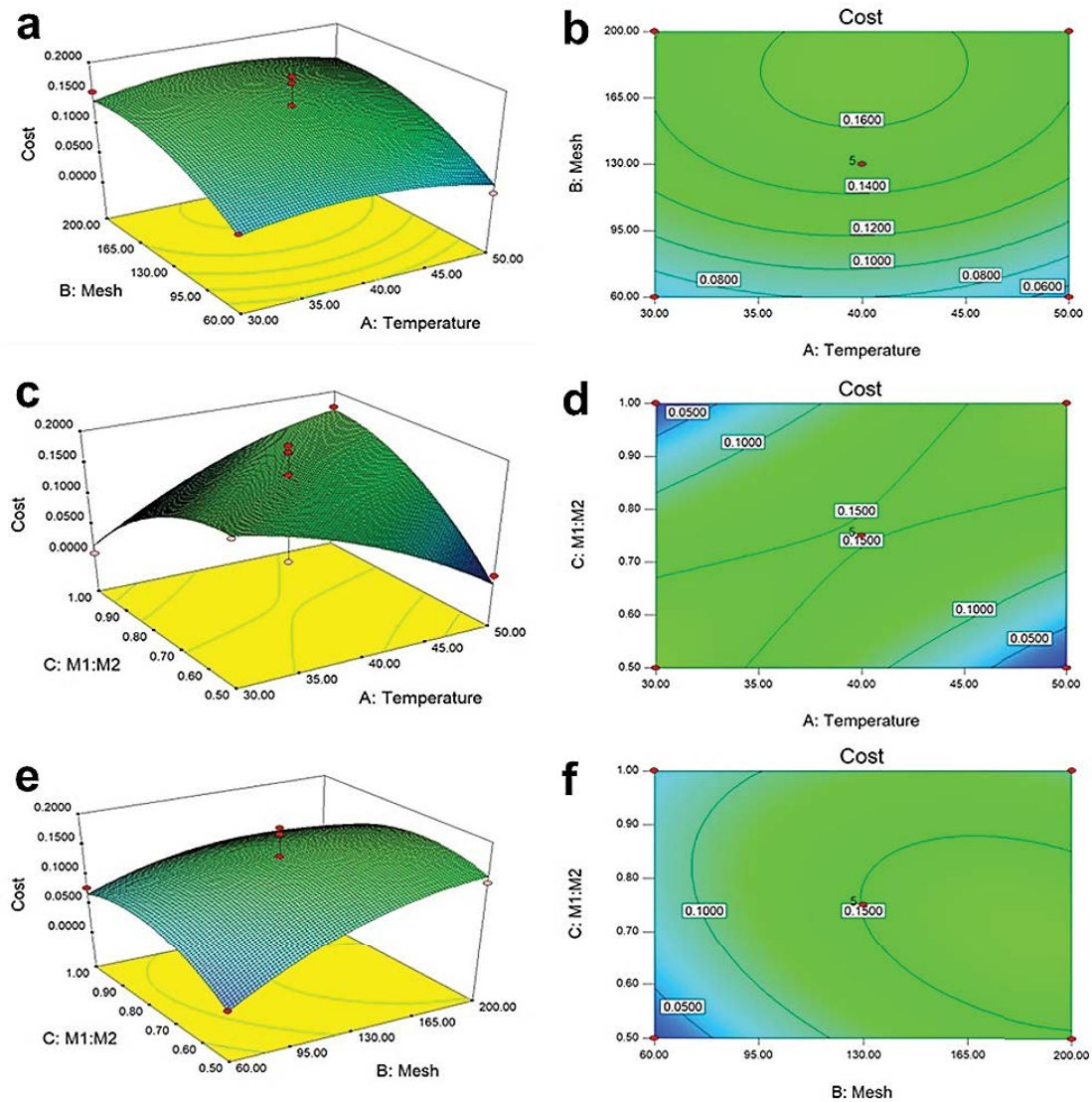
Fig. 2. Response surface map (a) and contour map (b) for the effect of reaction temperature and mesh; response surface map (c) and contour map (d) for the effect of reaction temperature and material ratio; response surface map (e) and contour map (f) for the effect of mesh and material ratio based on the cost.

the fixed reaction temperature at 40°C, respectively. The contour map was oval, and the axial contour for material ratio was dense while for material mesh was sparse, indicating that the material ratio had a more obvious impact on the cost. Under the optimal reaction conditions as follows: the material ratio was 0.75:1 and the material mesh was 120–200 mesh, the obtained cost was about 0.15.

As a whole, the process conditions for HACC grafting on the coconut shell-based skeleton particles were optimized by RSM, and the optimal process parameters were obtained as follows: reaction temperature at 40°C, material mesh at 120–200 mesh, and material ratio at 0.75:1, respectively. Under this process parameter, the actual consumption of HACC was measured at 0.1732 g/g, which was about 0.08 g/g different from the predicted value of the model. The results demonstrated that according to the Box–Behnken model, the grafting process of HACC obtained by response

surface analysis method was accurate and reliable, showing its potential development and utilization in the practical sludge disposal and other environmental field [40,41].

3.2. Performance evaluation of dewatering agent

Fig. 3a shows the dewatering performance of different dewatering agent. For three dewatering agents, the specific resistance and moisture content of sludge were basically decreased with the increasing dosage of dewatering agent. Under the dosage of 0.6 g/L, the specific resistance of sludge was 2.06, 0.98, and 0.34 10^9 s^2/g for PAC, CSBSP, GCSBSP, respectively. When the dosage of PAC increasing to 1.5 g/L, the specific resistance of sludge reached maximum, 0.92 10^9 s^2/g. Under the dosage of 0.6 g/L, the moisture content of sludge was 82.5%, 76.9%, and 71.3% for PAC, CSBSP, GCSBSP, respectively. When the dosage of PAC increasing

to 1.3 g/L, the moisture content could reach and maintain at minimum about 73.9%. Compared with the traditional dewatering material PAC, CSBSP and GCSBSP possess stronger

dewatering performance, with the minimum moisture contents at 78.2% and 70.4% for CSBSP and GCSBSP when the dosages were 0.5 g/L, respectively. Moreover, GCSBSP
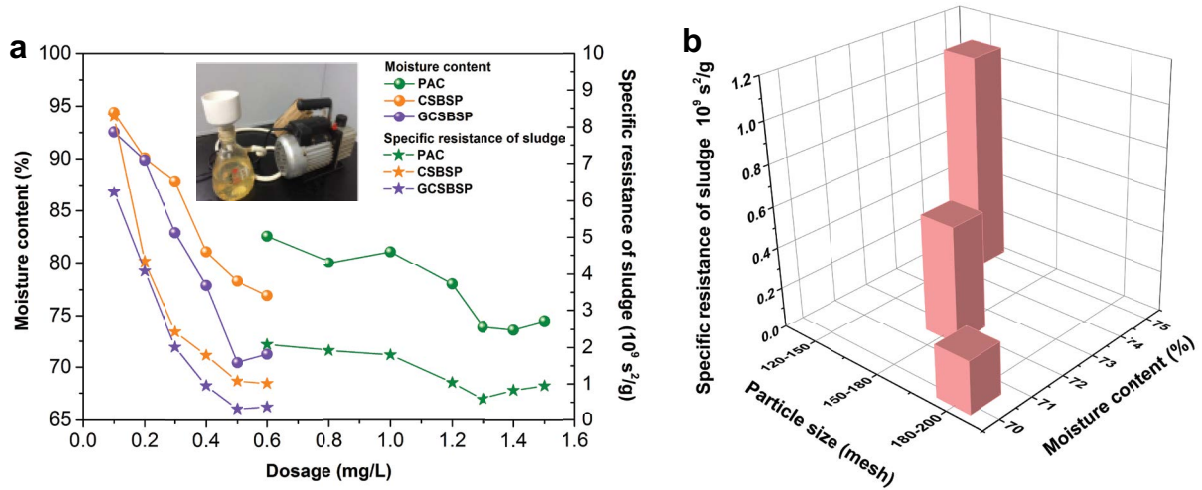

Fig. 3. Sludge specific resistance and moisture content of different dewatering agent (a); the effect of particle size of GCSBSP on dewatering performance (b).
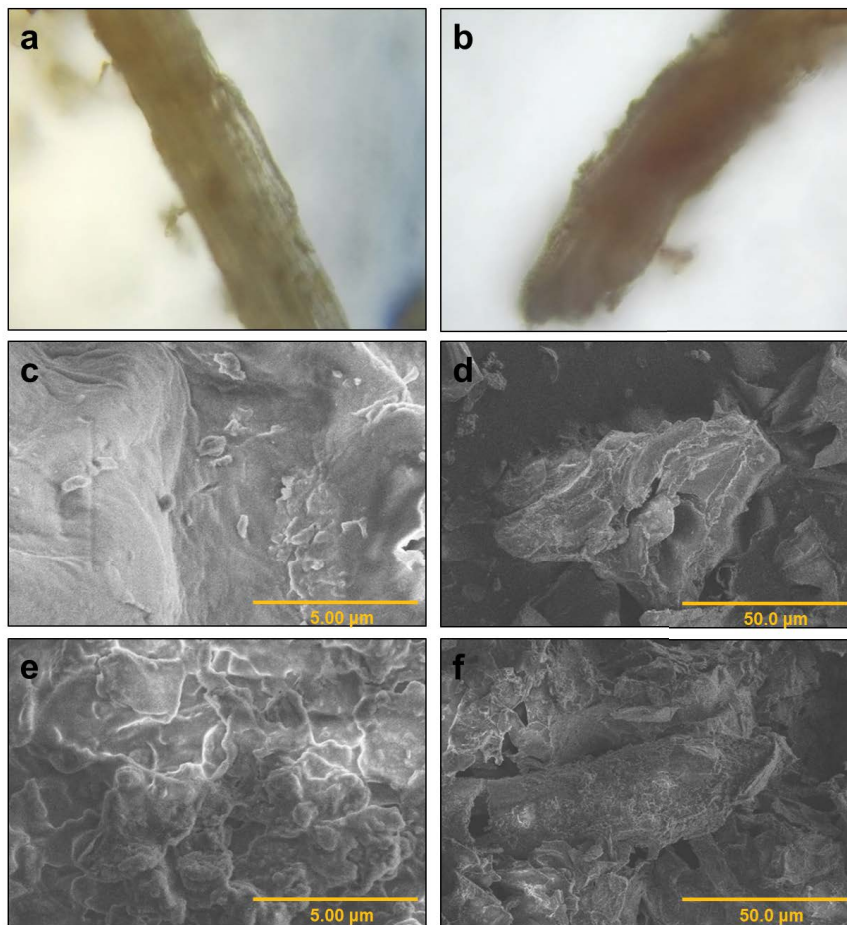

Fig. 4. Microscope magnification images (400-fold) of CSBSP (a) and GCSBSP (b); scanning electron microscopy images of CSBSP (c,d) and GCSBSP (e,f).

Table 4
Total nitrogen and total organic carbon removal test under different dewatering agent

Treated groups	Total nitrogen concentration in filtrate (mg/L)	Total organic carbon concentration in filtrate (mg/L)
Original	3.15 ± 0.21	5.26 ± 0.42
PAC (1.3 g/L)	3.04 ± 0.74	4.97 ± 0.17
CSBSP (0.5 g/L)	3.07 ± 0.45	4.63 ± 0.69
GCSBSP (0.5 g/L)	2.56 ± 0.98	2.79 ± 0.33
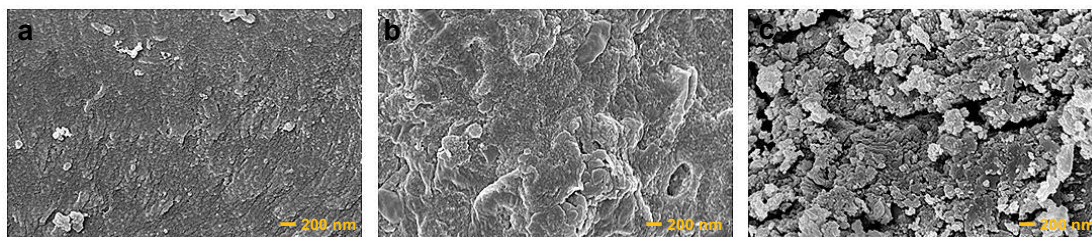
Fig. 5. Microscope magnification image of conditioned mud cake by dewatering agent: (a) PAC, (b) CSBSP and (c) GCSBSP.
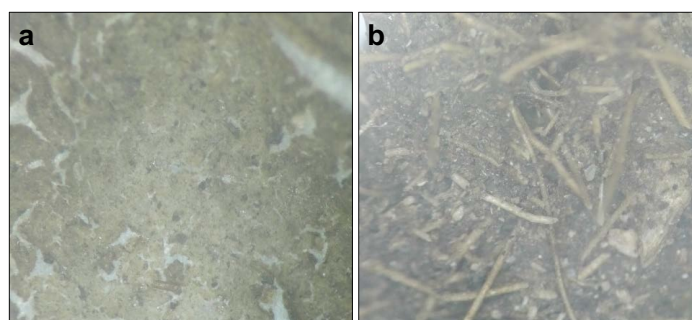

Fig. 6. Comparison of mechanical centrifugal dewatering status of activated sludge without GCSBSP (a) and with GCSBSP (b).

exhibited stronger dehydration performance than CSBSP, indicating the graft of HACC could effectively improve the sludge dewatering performance due to the flocculation effect of HACC [42,43]. Fig. 3b shows the effect of particle size of GCSBSP on dewatering performance. The result indicated small particle size (120–150 mesh) was conductive to the dewatering of sludge. The possible reason was due to small particle size of GCSBSP could provide more activation site for contact with sludge to enhance the dewatering performance. In addition, as for the contaminated matters removal in sludge contained wastewater, Table 4 shows the TOC and TN removal efficiencies using PAC, CSBSP, and GCSBSP, respectively. The addition of CSBSP and PAC possessed a poor removal effect on TN and TOC in the filtrate, while GCSBSP showed a certain removal efficiency on TN (18.7%) and TOC (47%) in the filtrate, ascribing to the adsorption effect on GCSBSP due to the HACC might enrich nitrogen and carbon sources on the surface [44].

3.3. Morphological characterization of CSBSP and GCSBSP

Fig. 4 shows the morphology characterization of CSBSP and GCSBSP using the optical microscope and scanning electron microscopy. It could be seen that CSBSP and GCSBSP exhibited an irregular fibrous structure with indistinct pore structure. Compared with CSBSP, the surface color of GCSBSP was darker and the surface structure of GCSBSP was rougher. The result of morphology characterization indicated the graft of HACC had no obviously affect on the structure and shape of CSBSP.

Fig. 5 shows microscope magnification image of conditioned mud cake by dewatering agent. The mud cake conditioned by PAC (Fig. 5a) had a smooth surface and a compact structure, and the agglomerate particles were firm, which was not conducive to the retention of water. The surface of the mud cake conditioned by CSBSP is uneven (Fig. 5b), and the appearance of voids was beneficial for water escaping. As seen in Fig. 5c, the mud cake conditioned by GCSBSP obviously had a large number of voids and flocculated particles independently, resulting in a higher dewatering efficiency. In addition, Fig. 6 shows the comparison of mechanical centrifugal dewatering status of activated sludge without and with GCSBSP, respectively. A part of the sludge was obviously adhered to the surface of GCSBSP, which could improve the dewatering rate of sludge. These results indicated that the application of GCSBSP was conducive to the sludge dewatering via both filtration and centrifuge methods.

4. Conclusion

In this study, a coconut shell-based grafted HACC composite material was novelty prepared. The RSM was used to optimize coconut shell-based grafted HACC at a temperature of 40°C, a material ratio of 0.75:1, a material mesh of 120–200 mesh, and under ultrasonic time of 5 min. The activated sludge conditioned by the coconut shell-based grafted HACC composite material showed a desired dewatering performance, and possessed the ability to effectively reduce the TOC and TN content in the sludge filtrate. This work provides a kind of eco-friendly biomass-derived skeleton particles for the municipal sludge conditioning and dewatering. In the further research, the pilot-scale test and practical application could be implemented using this GCSBSP composite materials to improving the sludge dewatering.

Author contribution statement

Shici Zhang and Ying Zhang: funding acquisition, investigation, methodology, conceptualization, experiment, data analysis, and writing original draft;

Haohan Xu and Qi Liu: experiment, data analysis, and writing review;

Xiang Wan: investigation, experiment, data analysis, and editing;

Jiajia Xia and Longkai Li: experiment and data analysis;

Hui Zhang: funding acquisition, data analysis;

Xujie Lu: project administration, supervision, conceived and designed the experiments.

Acknowledgements

Data availability

All data generated or analyzed during this study are included in this published article.

Ethics approval and consent to participate

The authors confirm that the manuscript has been read and approved by all authors. The authors declare that this manuscript has not been published and not under consideration for publication elsewhere.

Consent for publication

The authors consent to publish this research.

Competing interests

The authors have no relevant financial or non-financial interests to disclose.

References

[1] Y. Hu, F. Yang, F. Chen, Y. Feng, D. Chen, X. Dai, Pyrolysis of the mixture of MSWI fly ash and sewage sludge for co-disposal: effect of ferrous/ferric sulfate additives, Waste Manage., 75 (2018) 340–351.

[2] H. Luo, F. Cheng, B. Yu, L. Hu, J. Zhang, X. Qu, H. Yang, Z. Luo, Full-scale municipal sludge pyrolysis in China: design fundamentals, environmental and economic assessments, and future perspectives, Sci. Total Environ., 795 (2021) 148832, doi: 10.1016/j.scitotenv.2021.148832.

[3] H. Zhang, L. Rigamonti, S. Visigalli, A. Turolla, P. Gronchi, R. Canziani, Environmental and economic assessment of electro-dewatering application to sewage sludge: a case study of an Italian wastewater treatment plant, J. Cleaner Prod., 210 (2019) 1180–1192.

[4] J. Li, L. Liu, J. Liu, T. Ma, A. Yan, Y. Ni, Effect of adding alum sludge from water treatment plant on sewage sludge dewatering, J. Environ. Chem. Eng., 4 (2016) 746–752.

[5] H. Wei, B. Gao, J. Ren, A. Li, H. Yang, Coagulation/flocculation in dewatering of sludge: a review, Water Res., 143 (2018) 608–631.

[6] B. Cao, T. Zhang, W. Zhang, D. Wang, Enhanced technology based for sewage sludge deep dewatering: a critical review, Water Res., 189 (2021) 116650, doi: 10.1016/j.watres.2020.116650.

[7] X. Feng, J. Wan, J. Deng, X. Yue, Y. Yang, Z. He, X. Fang, T. Chen, S. Li, J. Lu, Y. Long, Study on the regulation of sludge dewatering by hydrophobically associating cationic polyacrylamide coupled with framework materials, J. Water Process Eng., 45 (2022) 102502, doi: 10.1016/j.jwpe.2021.102502.

[8] J. Qin, C. Zhang, Z. Chen, X. Wang, Y. Zhang, L. Guo, Converting wastes to resource: utilization of dewatered municipal sludge for calcium-based biochar adsorbent preparation and land application as a fertilizer, Chemosphere, 298 (2022) 134302, doi: 10.1016/j.chemosphere.2022.134302.

[9] X. Luo, M. Shen, J. Liu, Y. Ma, B. Gong, H. Liu, Z. Huang, Resource utilization of piggery sludge to prepare recyclable magnetic biochar for highly efficient degradation of tetracycline through peroxymonosulfate activation, J. Cleaner Prod., 294 (2021) 126372, doi: 10.1016/j.jclepro.2021.126372.

[10] C. Coskun, Z. Oktay, T. Koksal, B. Birecikli, Co-combustion of municipal dewatered sewage sludge and natural gas in an actual power plant, Energy, 211 (2020) 118615, doi: 10.1016/j.energy.2020.118615.

[11] D. He, M. Sun, B. Bao, J. Chen, H. Luo, J. Li, Rethinking the timing of flocculant addition during activated sludge dewatering, J. Water Process Eng., 47 (2022) 102744, doi: 10.1016/j.jwpe.2022.102744.

[12] H.-F. Wang, H. Hu, H.-J. Wang, R.J. Zeng, Impact of dosing order of the coagulant and flocculant on sludge dewatering performance during the conditioning process, Sci. Total Environ., 643 (2018) 1065–1073.

[13] Y. Qi, K.B. Thapa, A.F.A. Hoadley, Benefit of lignite as a filter aid for dewatering of digested sewage sludge demonstrated in pilot scale trials, Chem. Eng. J., 166 (2011) 504–510.

[14] K. Chen, Y. Sun, J. Fan, Y. Gu, The dewatering performance and cracking-flocculation-skeleton mechanism of bioleaching-coal fly ash combined process for sewage sludge, Chemosphere, 307 (2022) 135994, doi: 10.1016/j.chemosphere.2022.135994.

[15] R.H. Ramachandra, C.P. Devatha, Experimental investigation on sludge dewatering using granulated blast furnace slag as skeleton material, Environ. Sci. Pollut. Res., 27 (2020) 11870–11881.

[16] Q.X. Dai, N.Q. Ren, P. Ning, L.P. Ma, Z.Y. Guo, L.G. Xie, J. Yang, Y.Y. Cai, Inorganic flocculant for sludge treatment: characterization, sludge properties, interaction mechanisms and heavy metals variations, J. Environ. Manage., 275 (2020) 111255, doi: 10.1016/j.jenvman.2020.111255.

[17] X.R. Li, Y.F. Shi, X. Zhou, L. Wang, H.Q. Zhang, K.W. Pi, A.R. Gerson, D.F. Liu, Adaptability of organic matter and solid content to Fe^{2+}/persulfate and skeleton builder conditioner for waste activated sludge dewatering, Environ. Sci. Pollut. Res., 29 (2022) 14819–14829.

[18] J. Guo, Y. Zhou, Transformation of heavy metals and dewaterability of waste activated sludge during the conditioning by Fe^{2+}-activated peroxymonosulfate oxidation combined with rice straw biochar as skeleton builder, Chemosphere, 238 (2020) 124628, doi: 10.1016/j.chemosphere.2019.124628.

[19] H. Xiao, H. Liu, M. Jin, H. Deng, J. Wang, H. Yao, Process control for improving dewatering performance of sewage sludge based on carbonaceous skeleton-assisted thermal hydrolysis, Chemosphere, 296 (2022) 134006, doi: 10.1016/j.chemosphere.2022.134006.

[20] X. Wang, Y. Shen, X. Liu, T. Ma, J. Wu, G. Qi, Fly ash and H_2O_2 assisted hydrothermal carbonization for improving the nitrogen and sulfur removal from sewage sludge, Chemosphere, 290 (2022) 133209, doi: 10.1016/j.chemosphere.2021.133209.

[21] Y.Y. Jin, Y.Y. Li, F.Q. Liu, Combustion effects and emission characteristics of SO_2, CO, $NO_{(x)}$ and heavy metals during co-combustion of coal and dewatered sludge, Front. Environ. Sci. Eng., 10 (2016) 201–210.

[22] M.Q. Wang, Y. Wu, B.R. Yang, P.Y. Deng, Y.H. Zhong, C. Fu, Z.H. Lu, P.Y. Zhang, J.Q. Wang, Y.Y. Qu, Comparative study of the effect of rice husk-based powders used as physical conditioners on sludge dewatering, Sci. Rep., 10 (2020), doi: 10.1038/s41598-020-74178-7.

[23] J.L. Liang, J.J. Huang, S.W. Zhang, X. Yang, S.S. Huang, L. Zheng, M.Y. Ye, S.Y. Sun, A highly efficient conditioning process to improve sludge dewaterability by combining calcium hypochlorite oxidation, ferric coagulant re-flocculation, and walnut shell skeleton construction, Chem. Eng. J., 361 (2019) 1462–1478.

[24] S. Wang, Y.K. Yang, X.G. Chen, J.Z. Lv, J. Li, Effects of bamboo powder and rice husk powder conditioners on sludge dewatering and filtrate quality, Int. Biodeterior. Biodegrad., 124 (2017) 288–296.

[25] J. Guo, Q. Gao, S. Jiang, Insight into dewatering behavior and heavy metals transformation during waste activated sludge treatment by thermally-activated sodium persulfate oxidation combined with a skeleton builder–wheat straw biochar, Chemosphere, 252 (2020) 126542, doi: 10.1016/j.chemosphere.2020.126542.

[26] Z.Y. Guo, L.P. Ma, Q.X. Dai, R. Ao, H.P. Liu, J. Yang, Combined application of modified corn-core powder and sludge-based biochar for sewage sludge pretreatment: dewatering performance and dissipative particle dynamics simulation, Environ. Pollut., 265 (2020) 115095, doi: 10.1016/j.envpol.2020.115095.

[27] N. Rathnayake, S. Patel, P. Halder, S. Aktar, J. Pazferreiro, A. Sharma, A. Surapaneni, K. Shah, Co-pyrolysis of biosolids with alum sludge: effect of temperature and mixing ratio on product properties, J. Anal. Appl. Pyrolysis, 163 (2022) 105488, doi: 10.1016/j.jaap.2022.105488.

[28] R. Gabbrielli, F. Barontini, S. Frigo, L. Bressan, Numerical analysis of bio-methane production from biomass-sewage sludge oxy-steam gasification and methanation process, Appl. Energy, 307 (2022) 118292, doi: 10.1016/j.apenergy.2021.118292.

[29] S. Zhang, X. Lu, Treatment of wastewater containing Reactive Brilliant Blue KN-R using TiO_2/BC composite as heterogeneous photocatalyst and adsorbent, Chemosphere, 206 (2018) 777–783.

[30] Y. Xu, D.Y. Zhang, Q.J. Xue, C.B. Bu, Y.J. Wang, B.C. Zhang, Y. Wang, Q.D. Qin, Long-term nitrogen and phosphorus removal, shifts of functional bacteria and fate of resistance genes in bioretention systems under sulfamethoxazole stress, J. Environ. Sci., 126 (2023) 1–16.

[31] S. Edakkaparamban, M.S. Parasseri, G.K. Yogesh, C.B. Arumugam, S. Dillibabu, A simple nonenzymatic glucose sensor based on coconut shell charcoal powder-coated nickel foil electrode, Carbon Lett., 31 (2021) 729–735.

[32] H.R. Rashmi, C.P. Devatha, Dewatering performance of sludge using coconut shell biochar modified with ferric chloride (sludge dewatering using bio-waste), Int. J. Environ. Sci. Technol., 19 (2022) 6033–6044.

[33] M. Ebrahimi, K. Dunn, H. Li, D.W. Rowlings, I.M. O'Hara, Z. Zhang, Effect of hydrothermal treatment on deep dewatering of digested sludge: further understanding the role of lignocellulosic biomass, Sci. Total Environ., 810 (2022) 152294, doi: 10.1016/j.scitotenv.2021.152294.

[34] M.A. Babatabar, F. Yousefian, M.V. Mousavi, M. Hosseini, A. Tavasoli, Pyrolysis of lignocellulosic and algal biomasses in a fixed-bed reactor: a comparative study on the composition and application potential of bioproducts, Int. J. Energy Res., 46 (2022) 9836–9850.

[35] G. Tian, L. Li, B. Liu, T. Zhang, X. Hu, L. Zhang, B. Bian, Enhancing the dewaterability of the municipal sludge by flocculant combined with skeleton builder, Environ. Technol. Innovation, 25 (2022) 102166, doi: 10.1016/j.eti.2021.102166.

[36] H. Salehizadeh, N. Yan, R. Farnood, Recent advances in polysaccharide bio-based flocculants, Biotechnol. Adv., 36 (2018) 92–119.

[37] X. Lin, J. Liu, F. Zhou, Y. Ou, J. Rong, J. Zhao, Poly(2-hydroxyethyl methacrylate-co-quaternary ammonium salt chitosan) hydrogel: a potential contact lens material with tear protein deposition resistance and antimicrobial activity, Biomater. Adv., 136 (2022) 212787, doi: 10.1016/j.bioadv.2022.212787.

[38] J. Cao, G. He, X. Ning, X. Chen, L. Fan, M. Yang, Y. Yin, W. Cai, Preparation and properties of O-chitosan quaternary ammonium salt/polyvinyl alcohol/graphene oxide dual self-healing hydrogel, Carbohydr. Polym., 287 (2022) 119318, doi: 10.1016/j.carbpol.2022.119318.

[39] J. Guo, Q. Gao, Y. Chen, Q. He, H. Zhou, J. Liu, C. Zou, W. Chen, Insight into sludge dewatering by advanced oxidation using persulfate as oxidant and Fe^{2+} as activator: Performance, mechanism and extracellular polymers and heavy metals behaviors, J. Environ. Manage., 288 (2021) 112476, doi: 10.1016/j.jenvman.2021.112476.

[40] M.A. Tony, Y.Q. Zhao, J.F. Fu, A.M. Tayeb, Conditioning of aluminium-based water treatment sludge with Fenton's reagent: effectiveness and optimising study to improve dewaterability, Chemosphere, 72 (2008) 673–677.

[41] J. Rumky, M.C. Ncibi, R.C. Burgos-Castillo, A. Deb, M. Sillanpaa, Optimization of integrated ultrasonic-Fenton system for metal removal and dewatering of anaerobically digested sludge by Box–Behnken design, Sci. Total Environ., 645 (2018) 573–584.

[42] Q.J. Cai, S.H. Gong, K.Z. Song, P. Cai, C.C. Tian, C.B. Wang, M. Pan, B.D. Xiao, Effective harvesting of Scenedesmus using quaternary ammonium chitosan and xanthan gum: formation of mega flocs with oppositely charged polyelectrolytes, J. Cleaner Prod., 329 (2021) 129730, doi: 10.1016/j.jclepro.2021.129730.

[43] M. Huang, Z.Z. Liu, A.M. Li, H. Yang, Dual functionality of a graft starch flocculant: flocculation and antibacterial performance, J. Environ. Manage., 196 (2017) 63–71.

[44] Q. Wu, M.M. Gao, G.Y. Zhang, Y.H. Zhang, S.W. Liu, C.X. Xie, H.L. Yu, Y. Liu, L. Huang, S.T. Yu, Preparation and application performance study of biomass-based carbon materials with various morphologies by a hydrothermal/soft template method, Nanotechnology, 30 (2019) 185702, doi: 10.1088/1361-6528/ab0042.